Relevance of the steady laminar flamelet model for the large-eddy simulation of a reactive plume

Germain Boyer, Uday Chikkabikkodu, Javier Aguilera, Franck Richard, Arnaud Mura

▶ **To cite this version:**

Germain Boyer, Uday Chikkabikkodu, Javier Aguilera, Franck Richard, Arnaud Mura. Relevance of the steady laminar flamelet model for the large-eddy simulation of a reactive plume. EFSFF2024 - 4th European Symposium on Fire Safety Science, Oct 2024, Barcelona, Spain. pp.012053, 10.1088/1742-6596/2885/1/012053 . hal-04875715

HAL Id: hal-04875715
https://hal.science/hal-04875715v1

Submitted on 9 Jan 2025

HAL is a multi-disciplinary open access archive for the deposit and dissemination of scientific research documents, whether they are published or not. The documents may come from teaching and research institutions in France or abroad, or from public or private research centers.

L'archive ouverte pluridisciplinaire **HAL**, est destinée au dépôt et à la diffusion de documents scientifiques de niveau recherche, publiés ou non, émanant des établissements d'enseignement et de recherche français ou étrangers, des laboratoires publics ou privés.

Distributed under a Creative Commons Attribution 4.0 International License

Journal of Physics:
Conference Series

PURPOSE-LED PUBLISHING™

PAPER • OPEN ACCESS

Relevance of the steady laminar flamelet model for the large-eddy simulation of a reactive plume

To cite this article: Germain Boyer *et al* 2024 *J. Phys.: Conf. Ser.* **2885** 012053

View the article online for updates and enhancements.

You may also like

- High-accuracy multi-ion spectroscopy with mixed-species Coulomb crystals
J. Keller, H. N. Hausser, I. M. Richter et al.
- Prediction of the time to ignition of wood under transient heat exposure
Pauline Dias Lopes, Benjamin Batiot, Thomas Rogaume et al.
- Burning Rate and Carbon Monoxide Production for an elevated pool fire in a weakly ventilated compartment
E Georges, H Pretrel, K Varrall et al.

This content was downloaded from IP address 81.194.12.18 on 09/01/2025 at 06:42

Journal of Physics: Conference Series **2885** (2024) 012053 doi:10.1088/1742-6596/2885/1/012053

Relevance of the steady laminar flamelet model for the large-eddy simulation of a reactive plume

Germain Boyer[a], Uday Chikkabikkodu[a,b], Javier Aguilera[a], Franck Richard[b], Arnaud Mura[b]

[a] Institut de Radioprotection et de Sûreté Nucléaire (IRSN), PSN-RES/SA2I/LIE, Cadarache, St Paul Lez Durance 13115, France
[b] Institut Pprime, UPR 3346 CNRS, ENSMA et Université de Poitiers, Téléport 2 – 1 avenue Clément Ader, BP40109, 86961 Futuroscope Chasseneuil Cedex

E-mail: germain.boyer@irsn.fr

Abstract. The relevance of the steady laminar flamelet model (SLFM) is analyzed and discussed on the basis of computational results issued from the large-eddy simulation (LES) of a 30 cm diameter methanol pool fire. In a first step of the analysis, the computational results are assessed versus available experimental data: a satisfactory level of agreement is obtained. Then, the computational database is used to analyze the combustion regimes and model response.

1. Introduction and general context

In the purpose of developing and validating computational fluid dynamics (CFD) solvers dedicated to the simulation of fires in confined and ventilated conditions, reactive plumes are widely studied as reference canonical flows, insofar as they exhibit some of the typical features of fires such as buoyancy-driven dynamics, partially-developed or transitional turbulence, specific regimes of "turbulent" combustion, and combustion-radiation interactions. Even if the infinitely fast chemistry ("mixed is burnt") approach still remains widely used [1], the steady laminar flamelet model (SLFM) of Peters [2] has been rather recently retained as a another possible candidate to represent unresolved flow-chemistry interactions in the simulations of bench-scale fire experiments [3]. Indeed, this modeling approach does provide a suited framework to describe the chemical structure of the flame under the possible influence of flow motion (and associated strain-rate) and it can be readily generalized to take into account the influence of radiative losses on chemical species production, which may be of particular importance in under-oxygenated conditions [4].

In this context, the purpose of the present work is twofold. On the one hand, it aims at illustrating the capabilities of the SLFM approach – recently implemented within the CALIF^3-Isis software of IRSN [5] – to perform the large-eddy simulation (LES) of the methanol pool fires experimentally studied by Weckman *et al.* [6] and Hamins *et al.* [7–9]. On the other hand, the significant amount of computational data that is issued from this simulation is presently used in order to proceed with a detailed analysis of the characteristic scales and combustion regimes relevant to such reactive plumes.

Content from this work may be used under the terms of the Creative Commons Attribution 4.0 licence. Any further distribution of this work must maintain attribution to the author(s) and the title of the work, journal citation and DOI.
Published under licence by IOP Publishing Ltd

2. Numerical model

2.1. General features of the CFD solver

The present large-eddy simulation (LES) is carried out with the version 6.4 of the CALIF^{3}S-Isis software [5], previously used for the simulation of both non-reactive [10] and reactive [1] natural convection flows. This computational model is used to perform the resolution of the variable-density, Favre-filtered Navier-Stokes equations written within a low-Mach number formulation. Molecular fluxes are modeled with the Fourier and Fick laws with Soret and Dufour effects neglected. The Smagorinsky model is used in conjunction with the dynamic procedure to estimate the subgrid-scale (SGS) viscosity. The SGS fluxes are modeled on the basis of the turbulent diffusivity approximation with turbulent Prandtl and Schmidt numbers values set to 0.7. Radiative losses are taken into account through the resolution of the non-spectral radiative transfer equation (RTE) for an absorbing, non-scattering medium. The corresponding equation is solved within the finite volume framework using a discretization featuring 128 angular sectors. The radiative absorption includes the contributions of the gaseous combustion products H_2O and CO_2 through the non-spectral weighted sum of grey gases (WSGG) model.

2.2. Turbulent combustion modelling

The evolution of the composition is described within the SLFM framework [2] with the flame described as a collection of steady laminar strained diffusion flames, hereafter referred to as "flamelets". Thus, one-dimensional strained diffusion flames are computed for increasing values of the strain-rate until extinction is reached. In this regard, it is noteworthy that the strain-rate influence is parameterized in terms of the scalar dissipation rate (SDR) at stoichiometry $\mathrm{N}_{\xi_{st}}$. The corresponding flame structures (i.e., species mass fraction Y_α) are stored as functions of the mixture fraction ξ and SDR $\mathrm{N}_{\xi_{st}}$ in a look-up table $\mathcal{L}_l = \{Y_\alpha(\xi, \mathrm{N}_{\xi_{st}})\}$. On the basis of the corresponding set of data, the filtered composition may be deduced from:

$$\widetilde{Y}_\alpha\left(\widetilde{\xi}, \widetilde{\mathrm{S}}_\xi, \overline{\mathrm{N}}_{\xi_{st}}\right) = \int_\xi \int_{\mathrm{N}_{\xi_{st}}} Y_\alpha(\xi, \mathrm{N}_{\xi_{st}})\, \widetilde{\mathrm{P}}(\xi; \widetilde{\xi}, \widetilde{\mathrm{S}}_\xi)\, \mathrm{P}(\mathrm{N}_{\xi_{st}}; \overline{\mathrm{N}}_{\xi_{st}})\, \mathrm{d}\xi \mathrm{d}\mathrm{N}_{\xi_{st}} \tag{1}$$

where the quantities $\widetilde{\mathrm{P}}(\xi; \tilde{\xi}, \widetilde{\mathrm{S}}_\xi)$ and $\mathrm{P}(\mathrm{N}_{\xi_{st}}; \overline{\mathrm{N}}_{\xi_{st}})$ denote the mass-weighted (i.e., Favre) mixture fraction probability density function (PDF) and stoichiometric SDR PDF, respectively. In this respect, it must be emphasized that the above expression assumes statistical independence between mixture fraction and SDR. Morevover, the corresponding PDF are presumed on the basis of the first moments. Thus, based on the sole knowledge of the filtered value of the mixture fraction $\widetilde{\xi}$ and SGS normalized variance or segregation-rate $\widetilde{\mathrm{S}}_\xi = \widetilde{\mathrm{V}}_\xi / \widetilde{\xi}\left(1 - \widetilde{\xi}\right)$, with $\widetilde{\mathrm{V}}_\xi = \widetilde{\xi\,\xi} - \widetilde{\xi}\,\widetilde{\xi}$, the mixture fraction PDF $\widetilde{\mathrm{P}}(\xi)$ is evaluated using a Beta function whereas the stoichiometric SDR statistics $\mathrm{P}(\mathrm{N}_{\xi_{st}})$ is assumed to be a single Dirac delta peak at $\overline{\mathrm{N}}_{\xi_{st}}$, rather than a log-normal distribution with a unity standard deviation that is sometimes used instead. Thus, the filtered compositions, as given by Eq. (1), are stored as functions of the filtered values of scalar dissipation rate $\overline{\mathrm{N}}_{\xi_{st}}$, mixture fraction $\widetilde{\xi}$, and segregation-rate $\widetilde{\mathrm{S}}_\xi$ in another lookup table $\mathcal{L}_t = \left\{\widetilde{Y}_\alpha\left(\widetilde{\xi}, \widetilde{\mathrm{S}}_\xi, \overline{\mathrm{N}}_{\xi_{st}}\right)\right\}$. Accordingly, transport equations for the filtered mass fraction of chemical species $\widetilde{Y}_\alpha$ are not considered and, instead, transport equations are solved only for the filtered mixture fraction $\widetilde{\xi}$ and SGS variance $\widetilde{\mathrm{V}}_\xi$. The unresolved (i.e., SGS) SDR contribution that appears in the latter is represented with the linear relaxation model. Further details about the mixture fraction variance model may be found in the literature, see for instance Techer *et al.* [11]. Finally, the value of $\overline{\mathrm{N}}_{\xi_{st}}$ is approximated from the filtered SDR $\widetilde{\mathrm{N}}_\xi$ using the following expression $\widetilde{\mathrm{N}}_\xi \Big/ \int_\xi \mathrm{F}(\xi)/\mathrm{F}(\xi_{st})\widetilde{\mathrm{P}}(\xi)\, \mathrm{d}\xi$, which makes use of the flamelet SDR distribution function $\mathrm{F}(\xi) = \exp(-2\left[\mathrm{erf}^{-1}(1-2\xi)\right]^2)$.

2.3. Computational mesh and complementary computational details

Based on the plume injection diameter D = 30 cm of the NIST methanol pool fire [7–9], a 3D × 3D × 5D computational domain is used to proceed with the numerical simulation. It features the pool burner elevated at D/2 above the floor, including its five millimeter-thick lip. The grid is cartesian. The computational cell size Δ is chosen according to the LES quality requirement given by the Celik criterion [12], namely $\Delta \leq 25\eta_k$, with η_k the Kolmogorov length scale. This length scale is deduced from the turbulence integral length scale $\eta_k = \ell_t/\mathrm{Re}_t^{3/4}$ with $\mathrm{Re}_t = \sqrt{k}\,\ell_t/\nu$ the turbulent Reynolds number and with ℓ_t of the order of the plume diameter D. In this expression, the turbulent kinetic energy k is evaluated from $\mathrm{I}_t\mathrm{U}_a^2$ with I_t the turbulence intensity, of the order of 0.1, and with $\mathrm{U}_a = \sqrt{g\mathrm{D}}$ an estimate of the flow ascending velocity, which is typically of the order of 1 m/s. In these conditions, the Celik criterion implies that Δ must be of the order of D/40, a value that is presently retained as the reference grid cell size.

The conservation equations are discretized according to a marker and cell (MAC) staggered finite volume scheme. They are sequentially solved using a fractional step algorithm. For the momentum equation, the time derivative is approximated by a semi-implicit second-order Crank-Nicolson scheme and the convective operator is approximated thanks to a discrete kinetic-energy preserving second-order centered scheme. The convective operator involved in the scalar conservation equations is discretized using a third-order QUICK scheme. In practice, this combination of discrete operators leads to a CFL constraint on the time step δt, which is such that $\delta t = 0.05\Delta/\mathrm{U}_a$. The statistical averages presented in this work have been converged up to one percent, which has been achieved by retaining an integration time of 10 s.

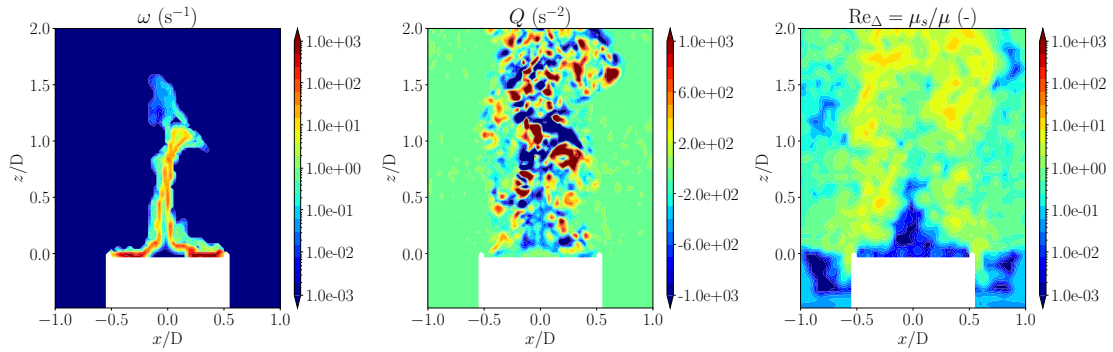

Figure 1: Instantaneous reaction rate (left), second invariant of the VGT (center), and local SGS Reynolds number (right), in the (x, z)-plane

3. Results and discussion

3.1. Reactive flow structure

The qualitative features of the computed flow are analyzed according to description of instantaneous values of the global reaction rate ω, the second invariant Q of the velocity gradient tensor (VGT), and the SGS Reynolds number $\mathrm{Re}_\Delta = \mu_s/\mu$, which are reported in Figure 1. In particular, the values of ω are deduced from the flamelet database:

$$\omega = \frac{1}{\overline{\rho}\Delta h_c} \sum_\alpha \Delta h^0_{f,\alpha} \widetilde{\omega}_\alpha \left(\widetilde{\xi}, \widetilde{\mathrm{S}}_\xi, \overline{\mathrm{N}}_{\xi_{st}}\right) \tag{2}$$

where Δh_c denotes the heat of combustion of the considered fuel, $\Delta h^0_{f,\alpha}$ is the enthalpy of formation of species α, and $\widetilde{\omega}_\alpha$ is its production/consumption rate as deduced from the lookup table $\mathcal{L}_t$. In the direct vicinity of the injection (i.e., $z <$ D), the SGS viscosity is negligible

(compared to the molecular one) and the vortical activity remains moderate. The flow is unsteady but far from being turbulent. An obviously laminar region is indeed found just downstream of the fuel injection and the corresponding zone features the largest chemical activity. In this respect, it seems worth emphasizing that, without requiring any low-Reynolds modification, the SLFM framework allows to recover the laminar flame limit in such conditions featuring vanishingly small turbulence intensity.

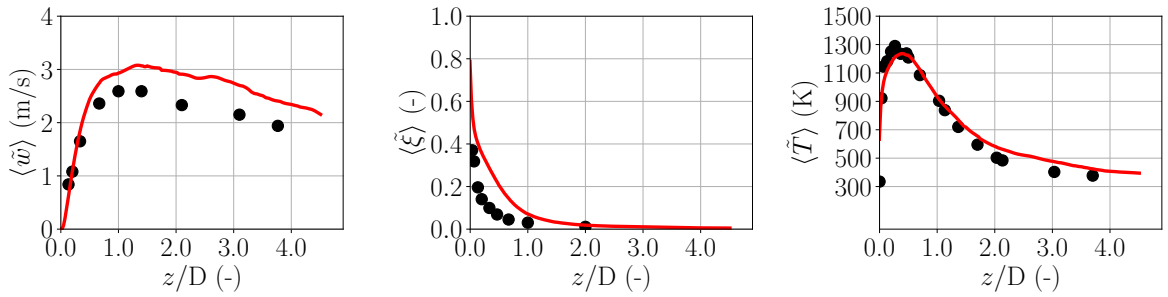

Figure 2: Axial evolution of averaged vertical velocity component, mixture fraction, and temperature obtained with the steady laminar flamelet model (—) and experimental measurements of Falkeinstein *et al.* [9, 13] (•).

From a more quantitative point of view, as observed in Figure 2, the computational model correctly reproduces the axial evolution of the averaged temperature and just slightly overestimates the axial velocity. In the radial direction (Figure 3), it underestimates the temperature in the range $0.2 < r/\mathrm{D} < 0.4$ and $z < \mathrm{D}$. The evolution that is observed on the experimental profiles of temperature is relevant to the the unsteady accumulation and ejection of light hot gases, which is associated to the plume puffing and Rayleigh-Taylor instabilities [14, 15]. In this respect, the main puffing frequency is correctly reproduced by the simulation: 2.85 Hz obtained by Fourier analysis of the velocity in the laminar core to be compared to 2.64 Hz in the experiments [9]. However, the underestimated levels of temperature observed for $0.2 < r/\mathrm{D} < 0.4, z < \mathrm{D}$ as well as the overestimated mixture fraction values on the symmetry axis (Figure 2), suggest that the unsteady mechanisms at play in the lower part of the plume are not fully resolved, and that, consequently, the grid resolution should be increased in the corresponding zone, insofar as a complex set of shear and buoyancy instabilities are expected to occur here [14, 15]. According to linear stability theory, the characteristic length of the most amplified perturbation scales as $\eta_{RT} = (\nu^2/g)^{1/3}$ and is of the order of $\eta_{RT} = 3 \times 10^{-4}$ m in the present case. The correct simulation of these phenomena would thus require a grid accuracy that

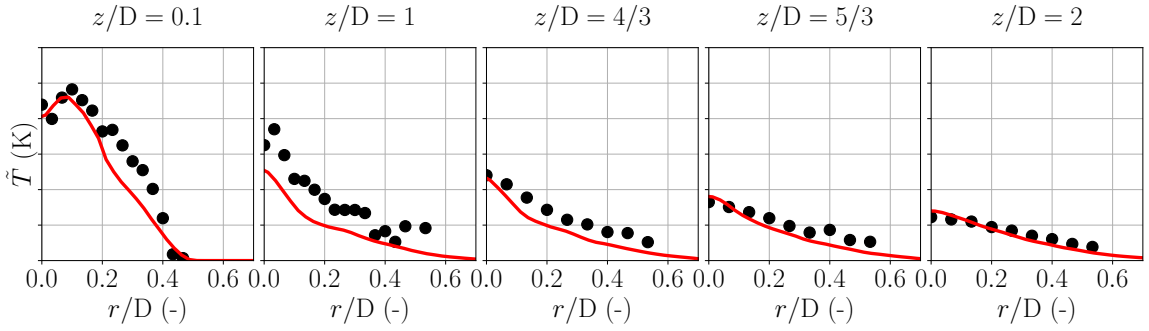

Figure 3: Radial evolution of the averaged temperature at heights $z/\mathrm{D} = \{0.1, 1, 4/3, 5/3, 2\}$ above the pool obtained with the steady laminar flamelet model (—) and experimental measurements of Hamins *et al.* [7, 8] (•).

approaches the DNS limit, which is by far unreachable to proceed with the numerical simulation of realistic fire plumes.

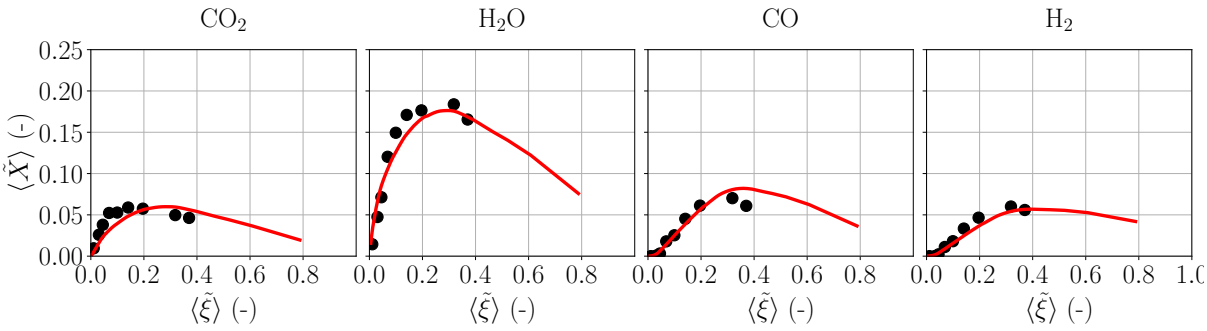

Figure 4: Axial evolution of the averaged mole fractions of combustion products obtained with the SLFM (—) and experimental measurements of Falkeinstein *et al.* [9] (•).

3.2. Steady laminar flamelet model and combustion regimes

The axial profiles of combustion products mole fractions, plotted versus $\widetilde{\xi}$, are reported in Figure 4. The quality of the obtained agreement between computational results and experimental measurements undoubtedly confirms the relevance of the SLFM framework for the present conditions.Then, the characteristic scales involved in this model, namely the turbulent scalar dissipation rate at stoichiometry $\overline{\mathrm{N}}_{\xi_{st}}$, SGS viscosity μ_s, turbulent time scale τ_t, and reaction rate ω, are analyzed. Thus, in Figure 5 are reported some plots of the reaction rate displayed in the planes $(\mathrm{Da}\,;\,\mathrm{Re}_\Delta)$ and $\left(\widetilde{\xi}\,;\,\overline{\mathrm{N}}_{\xi_{st}}/\mathrm{N}^q_{\xi_{st}}\right)$ with $\mathrm{N}^q_{\xi_{st}}$ the value of $\mathrm{N}_{\xi_{st}}$ at quenching (i.e., extinction). First, as emphasized in Section 3.1, the most significant part of chemical reactions takes place for values of Re_Δ that seldom exceeds unity: most of the chemical activity takes place at the resolved scale. Then, the local Damköhler number values $\mathrm{Da} = \overline{\mathrm{N}}_{\xi_{st}}/\omega$ remain always larger than unity (other definitions have been considered but are not discussed herein just for the sake of conciseness). Finally, at the resolved scale, the most reactive states are not relevant to stoichiometry but, instead, correspond to filtered mixture fraction values that lie between 0.25 and 0.35. The corresponding SDR values do not exceed $0.03\,\mathrm{N}^q_{\xi_{st}}$ and thus remain rather far from the strain-induced extinction limit. This confirms that the combustion regimes encountered in reactive plumes are much different from those met in more standard turbulent combustion conditions for which the dependency to the SDR is more significant.

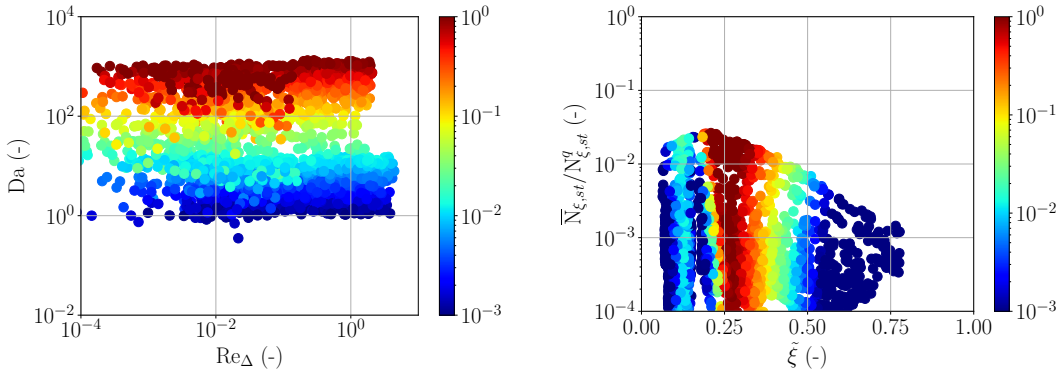

Figure 5: Local reaction rate ω plotted in the plane of local SGS Reynolds number and Damkhöler number (left) and in the plane of $\widetilde{\xi}$ and normalized SDR (right).

4. Conclusion and perspectives

Despite an under-estimated level of unsteady mixing in the quasi-laminar zone above the pool of fuel, the SLFM is confirmed to be suited to the simulation of such reactive plumes. The characteristic scales and combustion regimes are shown to be quite different from those relevant to higher Reynolds number flows that are typically used for the validation of such turbulent combustion models. According to recent recent attempts to apply the flamelet approach to the simulation of reactive plumes [16], further effort is now needed to incorporate (i) radiative losses effects on the chemical reactions and (ii) unsteady flamelet states that may result from radiation-induced extinction/re-ignition events, as typically observed in mechanically-ventilated compartment fires.

References

[1] G. Boyer, U. Chikkabikkodu, A. Mura, and F. Richard. Large-eddy simulation of a full-scale glove box fire. *Fire Safety J.*, 144:104101, 2024.

[2] N. Peters. Laminar diffusion flamelet models in non-premixed turbulent combustion. *Prog. Energy Combust. Sci.*, 10(3):319–339, 1984.

[3] V. M. Le, A. Marchand, S. Verma, R. Xu, J. White, A. Marshall, T. Rogaume, F. Richard, J. Luche, and A. Trouvé. Simulations of a turbulent line fire with a steady flamelet combustion model coupled with models for non-local and local gas radiation effects. *Fire Safety J.*, 106:105–113, 2019.

[4] H. Pretrel, L. Bouaza, and S. Suard. Multi-scale analysis of the under-ventilated combustion regime for the case of a fire event in a confined and mechanically ventilated compartment. *Fire Safety J.*, 120, 2021.

[5] Calif^{3}s collaborative website, 2024. URL `https://gforge.irsn.fr/#/project/calif3s`.

[6] E. J. Weckman and A. B. Strong. Experimental investigation of the turbulence structure of medium-scale methanol pool fires. *Combust. Flame*, 105(3):245–266, 1996.

[7] A. Hamins and A. Lock. The structure of a moderate-scale methanol pool fire. Technical Report 1928, NIST, 2016.

[8] K. Sung, R. Falkenstein-Smith, and A. Hamins. Velocity and temperature structure of medium-scale pool fires. Technical Report 2162, NIST, 2021.

[9] R. Falkenstein-Smith, K. Sung, J. Chen, and A. Hamins. Chemical structure of medium-scale liquid pool fires. *Fire Safety J.*, 120:103099, 2021.

[10] S. Vaux, R. Mehaddi, O. Vauquelin, and F. Candelier. Upward versus downward non-boussinesq turbulent fountains. *J. Fluid Mech.*, 867:374–391, 2019.

[11] A. Techer, Y. Moule, G. Lehnasch, and A. Mura. Mixing of fuel jet in supersonic crossflow: Estimation of subgrid-scale scalar fluctuations. *AIAA J.*, 56(2):465–481, 2018.

[12] I. B. Celik, Z. N. Cehreli, and I. Yavuz. Index of Resolution Quality for Large Eddy Simulations. *J. Fluids Eng.*, 127(5):949–958, 09 2005. doi: 10.1115/1.1990201.

[13] R. Falkenstein-Smith, K. Sung, J. Chen, K. Harris, and A. Hamins. The structure of medium-scale pool fires. Technical Report 2082, NIST, 2022.

[14] T. J. O'Hern, E. J. Weckman, A. L. Gerhart, S. R. Tieszen, and R. W. Schefer. Experimental study of a turbulent buoyant helium plume. *J. Fluid Mech.*, 544:143–171, 2005.

[15] F. Plourde, M. V. Pham, S. D. Kim, and S. Balachandar. Direct numerical simulations of a rapidly expanding thermal plume: structure and entrainment interaction. *Journal of Fluid Mechanics*, 604:99–123, 6 2008.

[16] R. Xu, V. M. Le, A. Marchand, S. Verma, T. Rogaume, F. Richard, J. Luche, and Trouvé. Simulations of the coupling between combustion and radiation in a turbulent line fire using an unsteady flamelet model. *Fire Safety J.*, 120:103101, 2021.